

RSC Applied Polymers

Accepted Manuscript

This article can be cited before page numbers have been issued, to do this please use: H. Shinohara, H. Araiara and H. Nishide, *RSC Appl. Polym.*, 2025, DOI: 10.1039/D4LP00336E.



This is an Accepted Manuscript, which has been through the Royal Society of Chemistry peer review process and has been accepted for publication.

Accepted Manuscripts are published online shortly after acceptance, before technical editing, formatting and proof reading. Using this free service, authors can make their results available to the community, in citable form, before we publish the edited article. We will replace this Accepted Manuscript with the edited and formatted Advance Article as soon as it is available.

You can find more information about Accepted Manuscripts in the [Information for Authors](#).

Please note that technical editing may introduce minor changes to the text and/or graphics, which may alter content. The journal's standard [Terms & Conditions](#) and the [Ethical guidelines](#) still apply. In no event shall the Royal Society of Chemistry be held responsible for any errors or omissions in this Accepted Manuscript or any consequences arising from the use of any information it contains.

ARTICLE

Highly Facilitated Permeation and Oxygen Enrichment from Air through Polyvinylimidazole Membrane Ligated with Kinetically Oxygen Interacting Cobaltporphyrin

Hiromi Shinohara,^{*a,b} Hirotsugu Araiara^a and Hiroyuki Nishide^{*a}Received 00th January 20xx,
Accepted 00th January 20xx

DOI: 10.1039/x0xx00000x

A dense and tough membrane of cobalt tetraphenylporphyrin (CoTPP) and poly(1-vinylimidazole-co-octyl methacrylate) (OIm) is prepared on a porous support. The oxygen permeability coefficient and oxygen/nitrogen permselectivity reach 10 Barrer and >110, respectively, at a pressure difference between the feed and permeate side of 2 cmHg. The membrane with a diameter of 10 cm enriches oxygen from dried air to an oxygen concentration > 60% through a one-shot permeation process. The reversible but kinetically very active interaction with oxygen molecules of the CoTPP fixed in the OIm membrane is analyzed for the membrane under a high oxygen pressure or low temperature with spectroscopies including laser-flash photolysis: i.e. >920 cmHg for the half of the CoTPP interacted with oxygen and extremely rapid oxygen-releasing rate constant of approximately 10^6 s^{-1} , extrapolated at room temperature. The enhanced oxygen diffusivity is discussed for the facilitated oxygen permeation through the membrane.

1. Introduction

Polymer membrane-based gas separation has been extensively investigated because of its energy-efficient and low-cost processes with a simple and high scalability.^{1–5} Practical examples of dense polymer membranes are composed of aromatic polyimides, polyethersulfones, and poly(vinylidene fluoride)s. Small gaseous molecule separation from mixed gases is based on the diffusivity of the permeate molecules by the difference in molecular diameter. The separation of hydrogen from its mixed gases, including a hydrogen/oxygen mixture produced by water splitting, has been recently highlighted.^{6,7} In contrast, the separation of condensed gases, such as carbon dioxide and nitrogen oxides, is mainly driven by the difference in gas solubility into the dense polymer membranes to achieve high permeability and permselectivity.

To separate gaseous molecules with similar physical characteristics, such as boiling point and molecular size, the properties of polymer membranes, including glass transition temperature (T_g) or free volume, are predominant in the gas permeation.⁸ For example, siloxane rubber is applied as a membrane for oxygen separation from air. However, the permselectivity of oxygen to nitrogen (P_{O_2}/P_{N_2}) remains as low as 2.⁹ In a progress article, Koros et al. recently reported that a semirigid polymer to mimic the rigid ultramicropore windows of

molecular sieves and zeolites is promising for a high permselectivity of P_{O_2}/P_{N_2} .¹⁰ Even in the case of poly(1-trimethylsilyl-1-propyne),¹¹ which has a rigid main chain and bulky side chain, its P_{O_2}/P_{N_2} remained low, 2–4, which suggests that it is difficult to attain a high permselectivity in the design of the molecular structures of polymers.

From another perspective, carrier-mediated transport or facilitated transport has been often investigated as a permselective membrane procedure.^{12–14} International Union of Pure and Applied Chemistry defines the “facilitated transport” process as chemically distinct carrier species bind with a specific component in the feedstream, thereby increasing the permeation of this component relative to other components.¹⁵ Facilitated transport with the carrier fixed into a dense membrane has been investigated to separate gaseous molecules, including oxygen from nitrogen.^{16,17} The carrier species were immobilized in the polymer membrane by maintaining their specific binding capability. Various carrier species to selectively bind and separate gaseous molecules have been reported. Representatives are cobalt(II) picketfence porphyrin^{18–20} with a cavity structure for a specific oxygen-coordinate site and cobalt(II) salcomines,^{21,22} which selectively bind molecular oxygen from air at room temperature. Another carrier species is monovalent silver (Ag^+) salts, which interact with olefins from olefin/paraffin^{23–27} and carbon monoxide from carbon monoxide/nitrogen²⁸ mixtures. These carriers fixed in the polymer matrix strongly bind the specific gaseous molecules to solubilize them within the membrane and yield a concentration gradient of the specific molecule as a driving force for selective permeation. The facilitated oxygen transport was successfully analyzed with a dual-mode transport model,^{16,17} i.e., linear combination of the contribution of

^a Research Institute for Science and Engineering, Waseda University, Tokyo 169-8555, Japan

^b Present Address: National Institute of Technology, Toyota Colledge, 2-1 Eisei-cho, Toyota, Aichi 471-8525, Japan

† Electronic supplementary information (ESI) available. See DOI: <https://doi.org/10.1039/x0xx00000x>



Langmuir-type adsorption of the specific molecule and physical permeation of the feed species.

In addition, simple, unmodified, and planar cobalt porphyrins and phthalocyanines have been reported as fixed carriers for the oxygen separation membranes.^{29–36} However, oxygen-binding capability of these simple cobalt porphyrins and phthalocyanines has not been recognized in inorganic and coordination chemistry,^{37,38} and, at least, the capability has not been verified under the conditions of permeation experiments. Moreover, the incorporation of the carrier molecules in the membrane influenced the physical properties of the membrane in some of these previous studies, which might make the permeation results unclear. Furthermore, the oxygen and nitrogen permeabilities have been measured with single-gas permeation experiments in the previous studies. The feasibility of the reported permselectivity is uncertain for practical separation of the oxygen and nitrogen mixed gases or, ultimately, air.

In this study, a dense and tough membrane was successfully prepared using a simple, planar, and cavity-free cobalt(II) tetraphenylporphyrin (CoTPP) as a fixed carrier and poly(vinylimidazole-co-octyl methacrylate) (OIm) as a polymer ligand. The ligation of imidazole moiety of OIm to the cobalt(II) ion forms the five-coordinated CoTPP, of which the sixth coordination site is vacant to possibly interact with an oxygen molecule. To optimize the balance between imidazole moiety content and membrane formability, octyl group was selected as alkyl group of the methacrylate in this study and the imidazole moiety content of OIm was determined to be 30 wt%. This allowed for the ligation of imidazole moiety even at high CoTPP concentrations and enabled the membrane to withstand permeation measurements at elevated pressures. The membrane was carefully coated on a porous support with nanometer thickness, and the obtained membrane was applicable to the feed side under a high pressure and easily scaled up to a large area. In addition, the physical properties of the CoTPP-incorporated membranes were maintained at the same rubbery state including a constant T_g with a constant physical nitrogen permeability coefficient, to quantitatively examine and clearly study the permeation results obtained with different membrane sizes and conditions. A membrane with a diameter of 10 cm was fabricated and oxygen enrichment from a dried air through a single-shot permeation process was demonstrated using a custom-made permeation apparatus. To discuss the function of the simple and planar CoTPP fixed in the OIm membrane in the oxygen permselectivity, the interaction of the CoTPP with oxygen was, for the first time, studied with rapid reaction spectroscopy and measurement under a high oxygen pressure. The mechanism of the oxygen facilitated permeation with the simple CoTPP fixed in the OIm membrane is discussed from the perspective of the kinetically very active fixed carrier.

2. Experimental Section

Materials

Cobalt(II) tetraphenylporphyrin (CoTPP) was purchased from Sigma-Aldrich. Cobalt(II) *meso- $\alpha,\alpha,\alpha,\alpha$ -tetrakis(o-pivalamidophenyl)porphyrin* (CoTpivPP) was synthesized as previously described.^{39,40} Polyacrylonitrile ultrafiltration membrane, obtained from GMT Membrantechtechnik was selected (see supporting information) as a porous support. 1-Vinylimidazole and octyl methacrylate were purchased from TCI and used after purification by distillation, with boiling points of 80 °C / 4 mmHg and 65 °C / 15 mmHg, respectively. Other solvents were purchased from Kanto Chem. and distilled prior to use.

Poly(1-vinylimidazole-co-octyl methacrylate) (OIm) was prepared via radical copolymerization. 1-Vinylimidazole (30 mL, 0.12 mol) and octyl methacrylate (42 mL, 0.18 mol) were added to a mixed solution of toluene (72 mL) and ethanol (48 mL) under a nitrogen atmosphere and reacted at 65 °C for 4 h with 2,2'-azobisisobutyronitrile (TCI, 0.06 mg, 37 mmol) as an initiator. The reaction mixture was poured into a large excess of methanol, and the precipitate was dissolved in a small amount of toluene and re-precipitated into methanol to obtain poly(1-vinylimidazole-co-octyl methacrylate) (24 g, 35 %) with a molecular weight of 1.3×10^5 with $M_w/M_n = 1.8$, and imidazole moiety content of 30 mol%, which were determined by gel permeation chromatography and elemental analysis, respectively.

Membrane preparation

OIm (3.7 mg) was thoroughly dissolved in THF (0.5 mL) overnight in a nitrogen-filled glove box. CoTPP (2.8 mg) was added and mixed to obtain the CoTPP-OIm solution. The solution was filtered through a PTFE membrane filter (Whatman Puradisc) with a pore size of 0.1 μm . The filtered solution was placed on a polyacrylonitrile porous support, carefully spread with a closely wound K bar (#0, wet film deposit height = 4 μm) in a glovebox using a K Hand coater (RK PrintCoat Instruments), and kept for 1 h under a nitrogen atmosphere. The membrane was then completely dried under vacuum to obtain the CoTPP-OIm coated membrane.

Permeation measurement for a single gas

The volumetric gas flow rates of oxygen and nitrogen at various feed gas pressures were measured using a self-made permeation apparatus with a soap-bubble flowmeter, as shown in Fig. S1. The feed pressure (p) range was 77–196 cmHg, while the permeate side pressure was atmospheric pressure: The pressure difference between the feed and permeate sides ($\Delta p = p - \text{atmospheric pressure (76 cmHg)}$). The permeability coefficient (P) was calculated from the volume of permeate (Q) and membrane thickness (l) obtained from the SEM image using eqn (1):

$$P = (Q \cdot l) / (\Delta p \cdot A \cdot t) \quad (1)$$



where A is the active area of the membrane and t is the time to obtain Q .

Permeation measurement for dried air (mixed oxygen/nitrogen gas)

The oxygen concentration on the permeate side was monitored by gas chromatography (Shimadzu GC-14B) using a gas sampler (10 mL) and He as the sweep gas (flow rate: 40 mL min⁻¹).

Oxygen permeability and enrichment from dry air using enlarged CoTPP-OIm membranes

A self-made gas permeation apparatus for a larger membrane (10 cm diameter) was assembled to measure the permeation volume with either a soap-bubble flowmeter or a flowmeter (Agilent ADM2000), and the oxygen concentration using a fluorescence oxygen analyzer (ASR F0-960). Dried air was used as the carrier gas.

Spectroscopic measurements

The interaction of oxygen with the CoTPP complexed with OIm was measured spectroscopically using a UV-vis spectrophotometer (V-550, JASCO) on the membrane cast on either the quartz window for the high-pressure cell or the quartz plate for the low-temperature measurement, with a thickness of approximately 1 μm . The oxygen binding kinetics were studied with a pulsed laser-flash spectrophotometer (FR-2000, Unisoku). The ESR spectrum of the deoxy CoTPP-OIm membrane was monitored with a JES-TE200ERS spectrophotometer (JEOL). A small piece of the dense membrane was packed in a quartz glass tube under an oxygen-free atmosphere at -77 K.

Other measurements

The cross-sectional view of the CoTPP-OIm was measured using a FE-SEM (JEOL S-2500CX, acceleration voltage: 25 kV). The surface topography of the CoTPP-OIm membrane was monitored using a tapping-mode AFM (Veeco Nanoscope IIIa). The T_g of the membranes was measured using differential scanning calorimetry (Seiko Instruments SSG/560U).

3. Results and Discussion

3.1. Membrane of the Cobaltporphyrin-Ligated Polyvinylimidazole and Highly Selective Oxygen Permeation

Membranes were prepared by coating the tetrahydrofuran solution of OIm and CoTPP upon a porous support, as illustrated in Fig. 1. A molar ratio of [imidazole moiety]/[CoTPP] = 1.67:1 (=42 wt% in CoTPP-OIm) and OIm concentration of the coating solution of 0.9 wt% were carefully selected to effectively ligate the imidazole moiety to CoTPP and avoid soaking of the CoTPP-OIm in the pore of the supporting membrane using bar coater, respectively (see supporting information, Table S1 and Fig. S2). The CoTPP-OIm-coated membrane was homogeneously light brownish in color. Surface scanning electron microscopy (SEM)

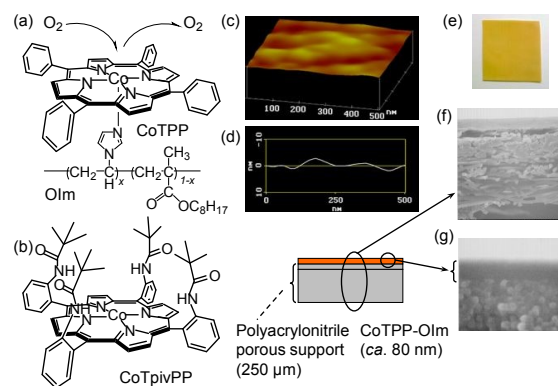


Fig. 1 Chemical structures of (a) cobalt tetraphenylporphyrin (CoTPP) and poly(vinylimidazole-co-octyl methacrylate) (OIm), and cobalt meso-tetra(α,α,α -o-pivalamidophenyl)porphyrin (CoTpiVPP). (c), (d) Atomic force microscopy images of the CoTPP-OIm membrane on a porous support. (e) Photograph of the CoTPP-OIm membrane on the porous support. (f), (g) Cross-sectional scanning electron microscopy images of the CoTPP-OIm membrane.

and atomic force microscopy (AFM) images supported smooth and pinholeless membrane formation. The cross-sectional SEM images indicate dense membrane formation with a thickness of approximately 80 nm on the porous support without filling the pores in the porous support. The membrane was mechanically robust, and the dense CoTPP-OIm membrane did not peel off or crack, even under high-pressure application during permeation measurements.

To provide a series of CoTPP-OIm membranes with similar physical properties, including glass transition temperature (T_g) and nitrogen permeability coefficient (P_{N_2}), the total CoTPP concentration incorporated in the OIm membrane was tuned constant at 42 wt%, by mixing the Co^ITPP, which interacts with molecular oxygen reversibly, with the Co^{III}TPP, which does not interact or is inactive to oxygen (Co^ITPP + Co^{III}TPP = constant 42 wt% in the membrane). T_g and P_{N_2} of the CoTPP-OIm membranes were maintained at approximately 6.0 °C and 0.09 Barrer (1 Barrer = 10⁻¹⁰ cm³ (STP) cm cm⁻² s⁻¹ cmHg⁻¹, = 3.35 × 10⁻¹⁶ mol m m⁻² s⁻¹ Pa in SI unit), respectively. The membrane thicknesses, T_g , and P_{N_2} of the series of CoTPP-OIm membranes with different active Co^ITPP contents using the permeation apparatus setup (Fig. S1) are listed in Table S2.

The P_{O_2} and P_{N_2} values of the CoTPP-OIm membranes were measured with a single-gas permeation process, and are presented in Fig. 2(a). P_{N_2} remained low and constant regardless of the feed nitrogen pressure. In contrast, P_{O_2} was higher than P_{N_2} , and increased steeply as the feed pressure decreased. P_{O_2} achieved 10.4 Barrer at a pressure difference between the feed and permeate side Δp ($= p - \text{atmospheric pressure (76 cmHg)} = 2 \text{ cmHg}$), and the oxygen permselectivity P_{O_2}/P_{N_2} reached 113 for the 42 wt% Co^ITPP membrane. As shown in the inset of Fig. 1, P_{O_2}/P_{N_2} increased with the Co^ITPP concentration. P_{O_2} of the Co^{III}TPP membrane (inactive Co^{III}TPP = 42 wt%) was low, even



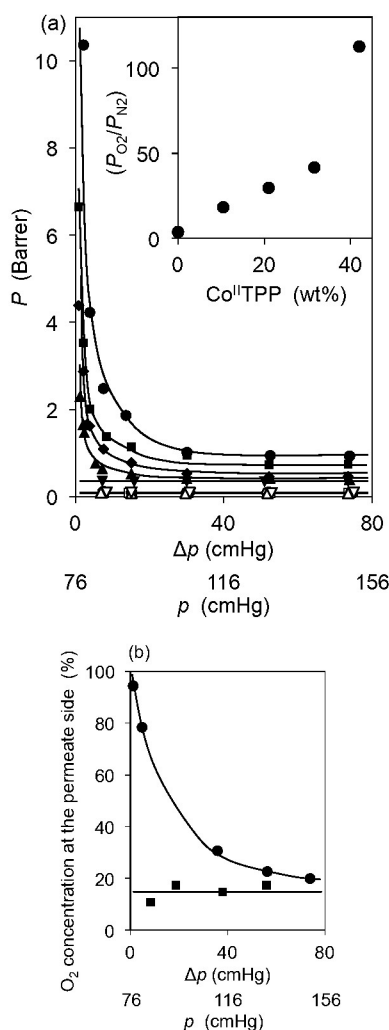


Fig. 2 (a) Single gas permeability coefficients (P) of oxygen and nitrogen at various feed pressures (p) for the CoTPP-OIm membranes. Δp = pressure difference between the feed and permeate sides ($\Delta p = p - \text{atmospheric pressure (76 cmHg)}$). $\text{Co}^{\text{II}}\text{TPP} + \text{Co}^{\text{III}}\text{TPP} = \text{constant } 42 \text{ wt\%}$. $[\text{Co}^{\text{II}}\text{TPP}] = 42$ (●), 32 (■), 21 (◆), 11 (▲), and 0 (▼) wt%, respectively. The T_g values of the membranes were maintained at ca. 6°C , as summarized in Table S2. Inset: Effect of the active $\text{Co}^{\text{II}}\text{TPP}$ content on O_2/N_2 permselectivity. (b) Oxygen concentration on the permeate side at various feed-air pressures for one-shot permeation through the $\text{Co}^{\text{II}}\text{TPP}$ - (●) and $\text{Co}^{\text{III}}\text{TPP}$ - (■) OIm membranes.

at low feed pressures, and remained constant regardless of the feed pressure. These results indicate that the CoTPP, as the fixed carrier in OIm, facilitates the oxygen permeation through the CoTPP-OIm membranes.

3.2. Reversible Oxygen Interaction to and its Kinetics of the CoTPP Fixed in the Polymer Membrane under a High Pressure or at a Low Temperature

Beforehand, ligation of the imidazole moiety of OIm and $\text{Co}^{\text{II}}\text{TPP}$ was examined with electron spin resonance (ESR) and ultraviolet

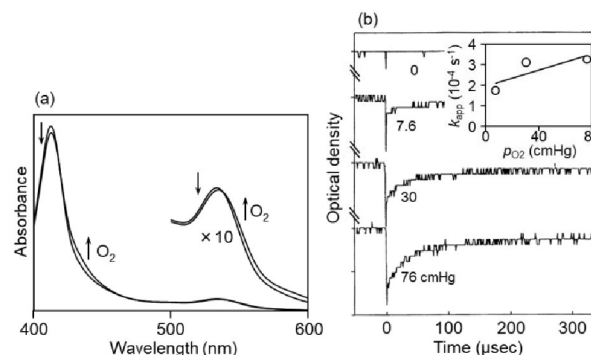
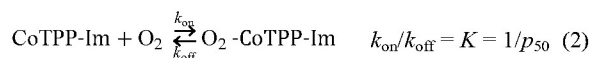


Fig. 3 (a) Visible absorption spectra of the CoTPP-OIm membrane at 25°C under oxygen at 0 and 7 atm. (b) Absorption recovery at 430 nm after laser flash irradiation at -15°C , ascribed to the recombination reaction of the photo-dissociated oxygen to the CoTPP complex of OIm in the solid membrane state under an oxygen partial pressure of 0 – 76 cmHg. Inset: Plots of apparent oxygen-binding rate constant (k_{app}) vs. oxygen partial pressures at -15°C .

(UV)–visible spectroscopy. The UV–visible spectrum of the $\text{Co}^{\text{II}}\text{TPP}$ with absorption maxima at 410 (Soret band) and 528 (Q band) nm was shifted to 412 and 530 nm, respectively, after the incorporation in the CoTPP-OIm membrane, which suggests the ligation of the imidazole moiety of OIm to $\text{Co}^{\text{II}}\text{TPP}$. The anisotropy in the ESR spectrum of the CoTPP-OIm membrane in an oxygen-free atmosphere at 77 K suggested that the $\text{Co}^{\text{II}}\text{TPP}$ was ligated with OIm and immobilized within the solid phase polymer. Eight hyperfine structures and three superfine structures in the ESR spectrum were ascribed to the nuclear spin quantum number of divalent cobalt (spin quantum number, $l = 7/2$) and to the nitrogen nucleus of a single imidazole moiety of OIm ligated to Co^{II} , respectively. Even a planar and cavity structure-free $\text{Co}^{\text{II}}\text{TPP}$ forms the five-coordinated $\text{Co}^{\text{II}}\text{TPP}$ -Im (Im: imidazole moiety). The imidazole ligation only at the fifth coordination site of Co remains the sixth site vacant to possibly interact with oxygen (Eqn (2)).

The selective and reversible interaction reaction of the $\text{Co}^{\text{II}}\text{TPP}$ ligated with the imidazole moiety of OIm with an oxygen molecule from air is expressed by



The interaction of the $\text{Co}^{\text{II}}\text{TPP}$ fixed in the OIm membrane was measured with visible absorption spectroscopy under a high oxygen pressure using a self-made high-pressure cell (Fig. S3). The two quartz windows were set in parallel, with the $\text{Co}^{\text{II}}\text{TPP}$ -OIm membrane coated on one window facing inside the cell.



Table 1 The oxygen partial pressure at which half of the cobaltporphyrin interacts with oxygen (p_{50}), and the oxygen-binding and releasing rate constants (k_{on} and k_{off}) of the cobaltporphyrins-OIm membranes extrapolated to 25 °C

Cobaltporphyrin	p_{50} (cmHg)	$10^{-7} k_{on}$ ($M^{-1} s^{-1}$)	$10^{-4} k_{off}$ (s^{-1})
CoTPP	920	5.0	860
CoTpivotPP ^[13a]	7.6	1.7	1.2

The assembly was then carefully sealed under a nitrogen atmosphere. The red-colored membrane yielded a visible absorption spectrum with $\lambda_{max} = 412$ and 530 nm, attributed to the deoxy CoTPP-Im,²⁹ in the absence of oxygen (Fig. 3(a)). Under a high-pressure oxygen gas (0–7 atm) application to the cell, the absorption at 430 and 547 nm, attributed to oxy CoTPP(Co/O₂ = 1/1 adduct, O₂-CoTPP-Im in Eqn (2)), increased with isosbestic points at 420 and 535 nm, in response to the oxygen pressure. After degassing inside the high-pressure cell, the CoTPP-OIm spectrum returned to its original deoxy form.

The spectral changes in the membrane were also measured at low temperatures with different oxygen partial pressures. The oxygen-binding equilibrium curves obeyed Langmuir isotherms to provide the oxygen-binding affinity p_{50} (the reciprocal of the equilibrium constant (K), the oxygen partial pressure at which half of the CoP interacts with oxygen). From the van't Hoff plot or temperature dependence of the logarithmic p_{50} , p_{50} was extrapolated to 920 cmHg for the CoTPP-OIm membrane at 25 °C, as shown in Table 1. The CoTPP-Im in the OIm membrane slightly binds oxygen at room temperature and enables a selective and reversible interaction with oxygen from air.

Photodissociation and recombination of the bound oxygen from and to the CoTPP-Im complex in a cooled OIm membrane were monitored by laser flash photolysis. The laser flash irradiation dissociates the bound oxygen from CoTPP-Im. The oxygen recombination time curve at -15 °C, monitored at the absorption maximum (430 nm) of O₂-CoTPP-Im in Eqn (2), is shown in Fig. 3(b), as an example. The spectral change ascribed to the recombination reaction was completed at approximately 100 μ s. It was very rapid despite the reaction in the solid-state membrane at a low temperature. The plots of the apparent oxygen-binding rate constant (k_{app}) vs. applied oxygen partial pressure were linear, which provided the oxygen-binding and -releasing rate constants (k_{on} and k_{off} in Eqn (2)) using pseudo-first-order kinetics, as shown in the inset of Fig. 3(b). From the Arrhenius plots of k_{on} and k_{off} , these values were extrapolated to obtain $5.0 \times 10^7 M^{-1} s^{-1}$ and $8.6 \times 10^6 s^{-1}$ at 25 °C, respectively, as shown in Table 1.

p_{50} , k_{on} , and k_{off} extrapolated to 25 °C for the CoTPP-Im fixed in the OIm membrane are listed in Table 1, with those of CoTpivotPP³⁹ (a picketfence porphyrin with a cavity structure on one side of the porphyrin plane, and benchmark cobaltporphyrin to reversibly bind an oxygen molecule at room

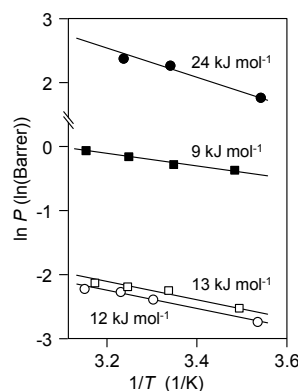


Fig. 4 Arrhenius plots of P_{O_2} (closed plots) and P_{N_2} (open plots) for the Co^{II}TPP (circle) and Co^{III}TPP (square) -OIm membranes.

temperature from air), also fixed in the OIm membrane. Compared to the values for the CoTpivotPP in the membrane, p_{50} was as extremely low as >920 cmHg (1.23 MPa) and k_{off} was significantly larger in the two digits for the CoTPP-OIm membrane. The CoTPP-Im is kinetically very active to interact with oxygen. The significantly large oxygen-releasing rate constant results in an extremely low oxygen-binding affinity. These results indicate that the very small oxygen-binding affinity and extremely rapid oxygen release from the CoTPP fixed in the OIm membrane are potentially the key factors for the high oxygen permeability with a high P_{O_2}/P_{N_2} .

3.3. Diffusivity and Solubility of Oxygen in the CoTPP-OIm Membranes

According to the oxygen sorption measurement, the oxygen sorption amount in the CoTPP-OIm membrane at 78 cmHg was 0.70 cm³ (STP) cm⁻³. This provided the molar ratio [dissolved oxygen]/[CoTPP] = ca. 1/20 for the 42 wt% CoTPP membrane even under 78 cmHg at 25 °C. In addition, a very large p_{50} (or very weak oxygen-binding affinity) of the CoTPP for the oxygen interaction indicates that the number of CoTPP bound with oxygen is less than one in 1000 even at an oxygen pressure of 76 cmHg. These results imply that most of the oxygen molecules in the membrane are physically dissolved. Their amount is considerably smaller than the amount of the CoTPP in the membrane under the conditions when the facilitated oxygen permeation was observed.

Damköhler number⁴¹ (Ψ), expressed by Eqn (3), is one of the nondimensional parameters used to compare the diffusivity via a chemical reaction and physical diffusivity.

$$\Psi = (k \cdot L^2 / D) \quad (3)$$

where L is the membrane thickness, D is the physical diffusion coefficient, and k is the first-order rate constant of the reaction, i.e., k_{off} , the oxygen-releasing rate constant in this study. D for the CoTPP-OIm membrane was estimated with the oxygen sorption amount and permeability coefficient of the 42 wt%



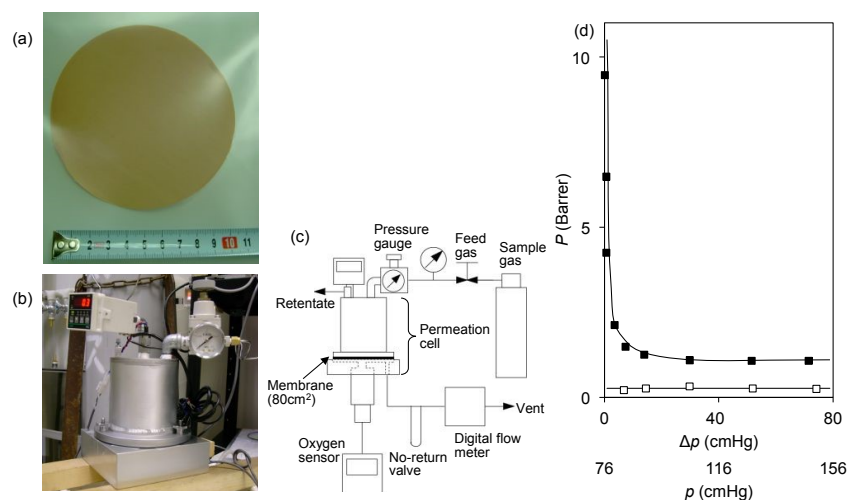


Fig. 5 (a) The CoTPP-Olm membrane for permeability measurement (10 cm diameter). (b) Photograph of the apparatus used for permeability measurement. (c) Flow diagram for the permeability measurement with larger size; Feed chamber size > 700 cm³, permeate chamber ca. 50 cm³. (d) Single gas permeability coefficients of O₂ (closed plots) and N₂ (open plots) at various feed pressures for the CoTPP-Olm membrane with 10 cm diameter. Δp = pressure difference between feed and permeate side ($\Delta p = p - p_{\text{atmospheric}}$ pressure (76 cmHg)).

Co^{III}TPP-Olm membrane to be $7.6 \times 10^{-8} \text{ cm}^2 \text{ s}^{-1}$. With these values, Ψ was calculated to be 7300, which implies that the chemical diffusion *via* the CoTPP as a fixed carrier in the membrane is significantly larger compared to the physical diffusion through the membrane. The temperature dependences of P_{O_2} and P_{N_2} for the 42 wt% Co^{III}TPP-Olm membrane were compared to those of the corresponding inactive Co^{III}TPP-Olm membrane, and are presented by $\ln(P_{\text{N}_2})$ vs. $1/T$ or Arrhenius plots in Fig. 4. membrane is significantly larger compared to the physical diffusion through the membrane. The activation energies (E_a) for the nitrogen permeation were 12 and 13 kJ/mol for the Co^{II} and the Co^{III}TPP membranes, respectively. E_a for the oxygen permeation through the control Co^{III}TPP membrane was 9 kJ/mol, slightly lower than that of nitrogen permeation, which was not inconsistent with the physical permselectivity of $P_{\text{O}_2}/P_{\text{N}_2} = 3.7$ for the membrane. On the other hand, E_a of P_{O_2} for Co^{II}TPP was 24 kJ/mol and significantly higher than those for the physical permeations of oxygen through the Co^{III}TPP membrane and of nitrogen through the Co^{II}TPP and Co^{III}TPP membranes. This result supports the contribution of the chemical reaction of the CoTPP fixed in the membrane, in addition to the physical permeation process, for the facilitated oxygen permeation. The distance of the CoTPP fixed in the Olm membrane was estimated with the size of the CoTPP molecule (approximately 1.3 nm). For the 42 wt% CoTPP membrane, the CoTPP molecules contact with each other and approximately 60 CoTPPs are packed and aligned in the direction of the membrane with a thickness of approximately 80 nm.

The above results conclude that the oxygen dissolved in the membrane is mainly due to a physical dissolution, and that the CoTPP, condensedly fixed in the membrane, selectively but very kinetically interacts with oxygen with an extremely high oxygen-

releasing rate and contributes to the significantly facilitated oxygen permeation through the membrane.

3.4. Oxygen Permeability and Enrichment from Dry Air Using Enlarged CoTPP-Olm Membranes

For a practical separation, dry air, a mixture of O₂ and N₂, is applied as a feed gas to examine oxygen enrichment with a single permeation through the CoTPP-Olm membrane, using the 42 wt% Co^{III}TPP-Olm membrane and corresponding Co^{III}TPP membrane as a control. The experimental setup for the measurement is illustrated in Fig. S1, while the oxygen concentration on the permeate side was analyzed with gas chromatography using helium as a carrier gas. Fig. 2(b) shows the permeate oxygen concentration at various feed air pressures (p). The oxygen concentration through the Co^{III}TPP-Olm membrane remained low and constant regardless of the feed air pressure. In contrast, the permeated oxygen concentration increased as the feed air pressure decreased, and the oxygen concentration reached 94% with a flow rate of 0.48 cm³ (STP) cm⁻² min⁻¹ at $p = 78.3$ cmHg. The oxygen concentration on the permeate side was calculated to be 98% based on the single-gas P_{O_2} and P_{N_2} in the previous section, which almost coincided with the oxygen enrichment performance from air using the same CoTPP-Olm membrane.

The CoTPP-Olm membrane with a larger area was prepared to support the oxygen enrichment result from air. Employing the same process for the smaller membrane, a pinholeless CoTPP-Olm-coated membrane with a diameter > 10 cm was prepared, as shown in Fig. 5(a). A permeation apparatus for the CoTPP-Olm membrane with a surface area of 80 cm² was designed to evaluate the gas permeability, as shown in Fig. 5(b) and (c). The feed side volume was set as large as possible (>700 cm³), and a



Table 2 Oxygen concentrations at permeate side $[O_2]$ at various feed pressures of dry air for the Co^{II} and Co^{III}TPP-OIm membranes with a large membrane in 10 cm diameter. Δp = pressure difference between feed and permeate side ($\Delta p = p - \text{atmospheric pressure}$ (76 cmHg))

Co ^{II} TPP	Δp	2	4	8	48	76
	(p)	(78)	(80)	(84)	(124)	(152)
	(cmHg)					
	$[O_2]$ (%)	61	62	49	38	38
Co ^{III} TPP	Δp			15	53	76
	(p)			(91)	(129)	(152)
	(cmHg)					
	$[O_2]$ (%)			35	36	35

fan was placed inside the feed side room to maintain the oxygen concentration of feed air constant during the permeation experiment. The volume of the permeation side was minimized to approximately 50 cm³ to sweep the permeated gas immediately to minimize back permeation. The permeate gas was monitored with the accommodated bubble flow meter and fluorescent oxygen sensor. The P_{O_2} and P_{N_2} values using single gases in this permeation process were measured, in advance, and compared with the results obtained for the previous small membrane, as shown in Fig. 5(d). P_{N_2} of the large membrane was almost the same as that of the smaller membrane, which indicates the validity of this permeation measurement. P_{O_2} was larger than P_{N_2} and extremely increased with the decrease in feed pressure, reaching 9.5 Barrer at Δp of 1 cmHg and P_{O_2}/P_{N_2} permselectivity of 50. These results indicate that a facilitated oxygen permeation through the CoTPP-OIm membrane was observed even for the membrane with a large area.

The oxygen concentrations detected on the permeate side through the Co^{II}TPP and Co^{III}TPP-OIm membranes for dry air application under pressure are summarized in Table 2. For the Co^{III}TPP membrane, the oxygen concentration remained low and was unaffected by the feed air pressure. On the other hand, the oxygen concentration definitely increased as the feed air pressure decreased for the Co^{II}TPP membrane permeation. An oxygen enrichment of approximately 60% was observed at an additional pressure of 2 cmHg at the feed air side with a flow rate of 60 mL min⁻¹ m⁻².

The P_{O_2} and P_{O_2}/P_{N_2} values measured for the CoTPP-OIm membrane in this study are extremely high, in comparison with those reported for polymer membranes⁴² (Fig. S4).

Conclusions

P_{O_2} reached 10 Barrer with a high oxygen permselectivity $P_{O_2}/P_{N_2} > 110$. The oxygen enrichment from air attained a value of approximately 60% for the polymer membrane of OIm ligated with the simple and planar 42 wt% CoTPP. This significantly facilitated oxygen permeation through the membrane was discussed with the selective but very kinetic oxygen interaction of the CoTPP carrier with an extremely high oxygen-releasing rate constant.

In addition, the CoTPP-OIm membrane was flexible and durable and was facile for preparation and scale-up in size. These features are promising for the membrane for testing in medical applications, air batteries, and other scenarios where oxygen-enriched air is needed.

Author contributions

H. S. and H. A. performed experimental work and H. S. and H.N. prepared the manuscript.

Conflicts of interest

There are no conflicts to declare.

Data availability

The data supporting this article has been included as part of the ESI. Data is available upon reasonable request from the authors.

Acknowledgements

This work was supported by KAKENHI from the Ministry of Education, Culture, Sports, Science and Technology, Japan.

References

- Y. Yampolskii, *Macromolecules*, 2012, **45**, 3298–3311.
- D. F. Sanders, Z. P. Smith, R. Guo, L. M. Robeson, J. E. McGrath, D. R. Paul and B. D. Freeman, *Polymer*, 2013, **54**, 4729–4761.
- S. Hasebe, S. Aoyama, M. Tanaka and H. Kawakami, *J. Membr. Sci.*, 2017, **536**, 148–155.
- R. Sidhikku Kandath Valappil, N. Ghasem and M. Al-Marzouqi, *J. Ind. Eng. Chem.*, 2021, **98**, 103–129.
- K. Cheng, K. Shinohara, O. Notoya, M. Teraguchi, T. Kaneko and T. Aoki, *Sep. Purif. Technol.*, 2024, **20**, 2308050.
- H. Nishide, *Green Chem.*, 2022, **24**, 4650–4679.
- H. Shinohara and H. Nishide, *Polym. Adv. Technol.*, 2024, **35**, e6524.
- R. S. Murali, T. Sankarshana and S. Sridhar, *Sep. Purif. Technol.*, 2013, **42**, 130–186.
- J. Brandrup and E. H. Immergut, Eds., *Polymer Handbook, 3rd Edition*, Wiley-Interscience, New York, 1989.
- W. J. Koros and C. Zhang, *Nature Mater.*, 2017, **16**, 289–297.
- T. Sakaguchi, Y. Hu and T. Masuda, in *Membrane Materials for Gas and Vapor Separation*, Y. Yampolskii and E. Finkelshtein Eds., John Wiley & Sons, Ltd, 2017, pp. 107–142.
- A. Figoli, W. F. C. Sager and M. H. V. Mulder, *J. Membr. Sci.*, 2001, **181**, 97–110.
- A. Matsuoka, E. Kamio, T. Mochida and H. Matsuyama, *J. Membr. Sci.*, 2017, **541**, 393–402.
- P. Luangrujiwong, A. Sungpet, J. D. Way and R. Jiratananon, *Ind. Eng. Chem. Res.*, 2006, **45**, 8213–8216.
- W. J. Koros, Y. H. Ma and T. Shimidzu, *Pure and Applied Chemistry*, 1996, **68**, 1479–1489.
- H. Nishide, M. Ohyanagi, O. Okada and E. Tsuchida, *Macromolecules*, 1986, **19**, 494–496.
- Hiroyuki. Nishide, Manshi. Ohyanagi, Osamu. Okada and Eishun. Tsuchida, *Macromolecules*, 1987, **20**, 417–422.
- H. Nishide, T. Suzuki, H. Kawakami and E. Tsuchida, *J. Phys. Chem.*, 1994, **98**, 5084–5088.



ARTICLE

Journal Name

- 19 H. Nishide, Y. Tsukahara and E. Tsuchida, *J. Phys. Chem. B*, 1998, **102**, 8766–8770.
- 20 B. Shentu and H. Nishide, *Ind. Eng. Chem. Res.*, 2003, **42**, 5954–5958.
- 21 E. Tsuchida, H. Nishide, M. Ohyanagi and H. Kawakami, *Macromolecules*, 1987, **20**, 1907–1912.
- 22 W. Choi, P. G. Ingole, H. Li, S. Y. Park, J. H. Kim, H.-K. Lee and I.-H. Baek, *Microchem. J.*, 2017, **132**, 36–42.
- 23 S. Sunderrajan, B. D. Freeman, C. K. Hall and I. Pinnau, *J. Membr. Sci.*, 2001, **182**, 1–12.
- 24 J. H. Kim, B. R. Min, C. K. Kim, J. Won and Y. S. Kang, *Macromolecules*, 2002, **35**, 5250–5255.
- 25 J. H. Kim, B. R. Min, J. Won, S. H. Joo, H. S. Kim and Y. S. Kang, *Macromolecules*, 2003, **36**, 6183–6188.
- 26 C. Yu, M. G. Cowan, R. D. Noble and W. Zhang, *Chem. Commun.*, 2014, **50**, 5745–5747.
- 27 J. P. Jung, C. H. Park, J. H. Lee, J. T. Park, J.-H. Kim and J. H. Kim, *J. Membr. Sci.*, 2018, **548**, 149–156.
- 28 N. U. Kim, J.-H. Kim, B. R. Park, K. C. Kim and J. H. Kim, *J. Membr. Sci.*, 2021, **620**, 118939.
- 29 H. Shinohara, T. Arai and H. Nishide, *Macromol. Symp.*, 2002, **186**, 135–139.
- 30 H. Shinohara, A. Nakao and H. Nishide, *Kobunshi Ronbunshu*, 2002, **59**, 656–660.
- 31 H. Shinohara, H. Shibata, D. Wöhrle and H. Nishide, *Macromol. Chem. Phys.*, 2005, **206**, 467–470.
- 32 N. Preethi, H. Shinohara and H. Nishide, *React. Funct. Polym.*, 2006, **66**, 851–855.
- 33 M. Shoji, K. Oyaizu and H. Nishide, *Polymer*, 2008, **49**, 5659–5664.
- 34 N. Chikushi, E. Ohara, A. Hisama and H. Nishide, *Macromol. Rapid Commun.*, 2014, **35**, 976–980.
- 35 H. Nagar, P. Vadthya, N. S. Prasad and S. Sridhar, *RSC Adv.*, 2015, **5**, 76190–76201.
- 36 H. Li, W. Choi, P. G. Ingole, H. K. Lee and I. H. Baek, *Fuel*, 2016, **185**, 133–141.
- 37 E. Tsuchida and H. Nishide, *Top. Curr. Chem.*, 1986, **132**, 63–99.
- 38 D. Wöhrle and A. D. Pomogailo, Eds., *Metal Complexes and Metals in Macromolecules: Synthesis, Structure and Properties*, Wiley-VCH GmbH, Weinheim, 2003.
- 39 J. P. Collman, R. R. Gagne, C. Reed, T. R. Halbert, G. Lang and W. T. Robinson, *J. Am. Chem. Soc.*, 1975, **97**, 1427–1439.
- 40 J. P. Collman, J. I. Brauman, K. M. Doxsee, T. R. Halbert, S. E. Hayes and K. S. Suslick, *J. Am. Chem. Soc.*, 1978, **100**, 2761–2766.
- 41 C. Weiland, in *Mechanics of Flow Similarities*, ed. C. Weiland, Springer, Cham, 2020, pp. 39–50.



Data Availability Statement

Highly Facilitated Permeation and Oxygen Enrichment from Air through Polyvinylimidazole Membrane Ligated with Kinetically Oxygen Interacting Cobaltporphyrin

*Hiromi Shinohara**, *Hirotsugu Araiara*, and *Hiroyuki Nishide**

The data supporting this article has been included as part of the ESI. Data is available upon reasonable request from the authors.

